

1 Preparation and characterization of esterified bamboo flour

2 by an *in situ* solid phase method

3 Yaqi Geng^a, Xiaohan Pei^a, Xiaoyu He^a, Ping Li^a, Yiqiang Wu^{a,b}, Yingfeng Zuo^{a,b*}

4 ^a College of Materials Science and Engineering, Central South University of Forestry and
5 Technology, Changsha 410004, PR China

6 ^b Hunan Provincial Collaborative Innovation Center for High-efficiency Utilization of Wood and
7 Bamboo Resources, Central South University of Forestry and Technology, Changsha 410004,
8 PR China

9 *Corresponding author

10 Yingfeng Zuo (Y. Zuo)

11 Affiliation: College of Materials Science and Engineering, Central South University of Forestry
12 and Technology, Changsha, Hunan 410004, PR China

13 Email address: zuoyf1986@163.com

14 Phone number: +86 731 85623301

15 Fax: +86 731 85623301

16 **Abstract:** Bamboo plastic composites have become a hot research topic and a key focus of
17 research. However, the many strong, polar, hydrophilic hydroxyl groups in bamboo flour (BF)
18 results in poor interfacial compatibility between BF and hydrophobic polymers. Maleic
19 anhydride-esterified (MAH-e-BF) and lactic acid-esterified bamboo flour (LA-e-BF) were
20 prepared using an *in situ* solid-phase esterification method with BF as the raw material and maleic
21 anhydride or lactic acid as the esterifying agent. Fourier transform infrared spectroscopy results
22 confirmed that BF esterification with maleic anhydride and lactic acid was successful, with the
23 esterification degrees of MAH-e-BF and LA-e-BF at 21.04 and 14.36%%, respectively. Esterified
24 BF was characterized by scanning electron microscopy, contact angle testing, X-ray diffractometry,
25 and thermogravimetric analysis. The results demonstrated that esterified BF surfaces were covered
26 with graft polymer and the surface roughness and bonding degree of MAH-e-BF clearly larger
27 than those of LA-e-BF. The hydrophobicity of esterified BF was significantly higher than BF and
28 the hydrophobicity of MAH-e-BF better than LA-e-BF. The crystalline structure of esterified BF
29 showed some damage, with MAH-e-BF exhibiting a greater decrease in crystallinity than LA-e-BF.

30 Overall, the esterification reaction improved BF thermoplasticity, with the thermoplasticity of
31 MAH-e-BF appearing better than LA-e-BF.

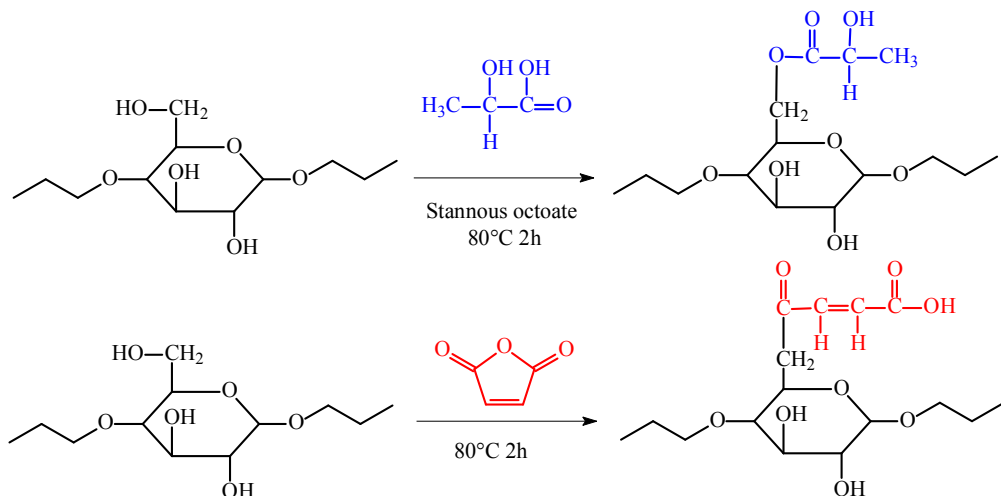
32 **Keywords:** bamboo flour; in situ solid phase method; esterification modification; substituting
33 degree; hydrophobicity

34 **1. Introduction**

35 In China, bamboo is a rich resource, having the benefit of a short growth cycle, and research
36 into and utilization of bamboo have attracted much attention [1,2]. Various kinds of bamboo
37 wood-based panels, active carbon, and fuel have been successfully developed [3,4]. However,
38 these traditional processing methods have low utilization rates, high energy consumption, serious
39 pollution issues, lack of effective utilization, single performance uses, and low added value. If
40 bamboo leftovers from these processes and bamboo plastic composite polymer mixed preparations
41 can be used for packaging, construction, and even used in cars, high-speed rail, aircraft, floors,
42 and interiors, it would not only effectively improve the utilization rate of bamboo timber and
43 produce added value, but it would also promote the development of a circular economy and help
44 maintain an ecological balance [5,6].

45 However, there are many strong, polar, hydrophilic hydroxyl groups in bamboo, which are
46 incompatible with polymer interfaces and directly affect the thickness, morphology, structure, and
47 dispersion uniformity of the material, leading to deterioration of material properties. Therefore,
48 reducing the hydrophilic groups in bamboo and replacing hydrophobic -OH with hydrophilic
49 groups is an effective way to improve bamboo hydrophobicity. The methods for modifying
50 bamboo hydrophobicity, using existing technology, includes bamboo fiber steam explosion [7,8]
51 and electron beam irradiation. These physical methods can improve the mechanical interlocking
52 forces of BF and polymer composites to a certain extent, but they cannot form a strong chemical
53 bond between the fiber and resin matrix. For this reason, researchers have used chemical methods
54 to modify these plant fibers. Bledzki has pointed out that a fiber-coupling agent treatment can
55 change fiber wettability and improve the interfacial compatibility of composite materials [9].
56 However, this method generally requires modification by a coupling agent in an organic solvent,
57 which increases production costs and also has potential to damage the environment. Also, Lee has
58 studied maleic anhydride (MAH)-esterified bamboo fiber compounded into a composite material,
59 which improved interfacial compatibility [10]. In addition, many studies have used esterification

60 reactions to modify BF and achieved good results [11,12].



61
62 **Fig.1 Reaction mechanism of esterified BF**

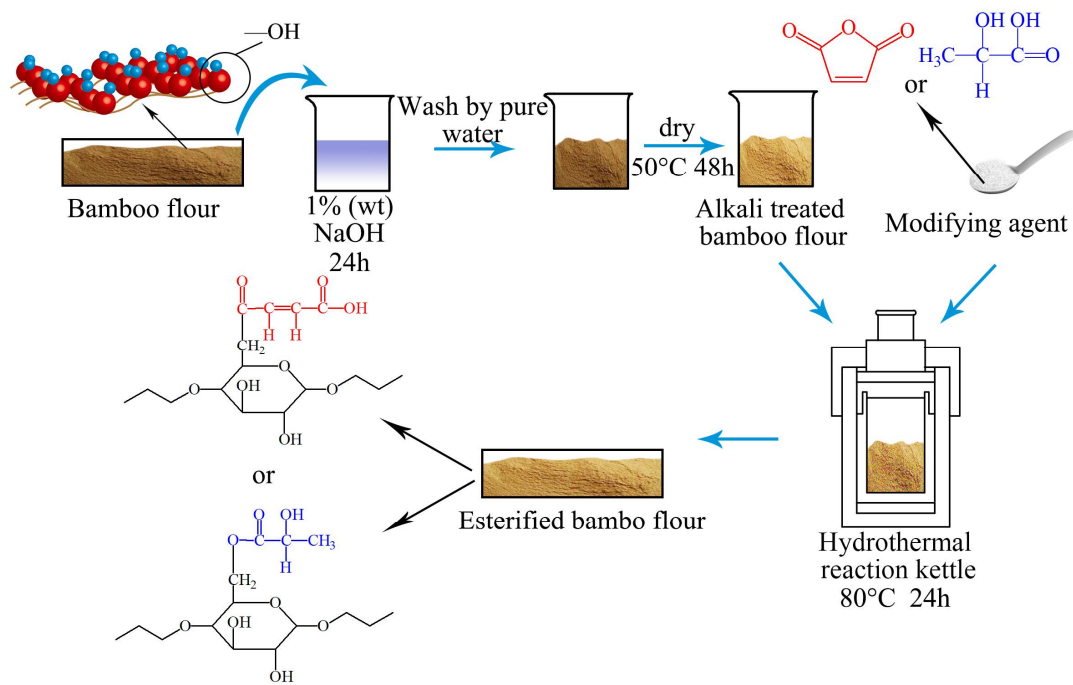
63 Chemical modification of the plastic matrix has been shown to form a molecular/structural
64 bridge between the fibers and plastic, which is conducive to enhancing the bonding between
65 interfaces. At present, the most commonly used esterification methods include an aqueous phase,
66 organic solvent, and reactive extrusion methods. The water phase method is a uniform reaction
67 and no organic solvent is required but, because the reaction is a heterogeneous reaction between
68 the solid particles of BF and the liquid, the affinity and forces between the two reactants are not
69 high and hydrolysis of carboxylic acid is a side reaction. The organic solvent reaction is uniform,
70 but the degree of substitution is not high and the reaction has environmental pollution problems.
71 The reaction extrusion method needs plasticizer, which destroys the BF particle structure and
72 restricts the range of BF applications. In view of this, a solid-phase esterification method *in situ*
73 was used to modify bamboo. Lactic acid (LA) and MAH belong to two carboxylic acids, and their
74 use to modify BF can improve its crosslinked structure. In experiments here, BF was mixed with
75 LA or MAH in an airtight reactor and the solid phase esterification reaction carried out under
76 certain pressure and temperature conditions (Fig.1). Compared with solution and melting
77 condensation polymerization, solid phase esterification exhibited the following advantages: (1) the
78 reaction temperature was significantly reduced and by-products and degradation reactions also
79 reduced; (2) the monomer concentration was large and fully reacted, the reaction was favored, and
80 the reaction efficiency high; (3) the condensation reaction was stable and high pressure not
81 required; (4) the reaction system did not require organic solvents. This was overall an

82 environmentally-friendly condensation process. This *in situ* solid-phase esterification of BF was
 83 found to be a highly efficient and environmentally-friendly process.

84 **2. Materials and Methods**

85 **2.1 Materials**

86 The BF used in this study was supplied by Hunan Taohuajiang Industrial Co., Ltd. (Yiyang,
 87 Hunan, China) and used as received. LA was obtained from Chongqing East Sichuan Chemical
 88 Co., Ltd. (Jiguanshi Town, China). MAH was purchased from Tianjin Kemiou Chemical Reagent
 89 Co., Ltd. (Tianjin, China). Acetone was obtained from Hunan Normal University Chemical
 90 Reagent Factory (Changsha, China). Sodium hydroxide was obtained from Xilong Chemical Co.,
 91 Ltd. (Guangzhou Science City, China). Ethanol (99.7%) was obtained from Anhui Ante Food Co.,
 92 Ltd. (Anhui, China). All chemicals were reagent grade. Ultrapure water was obtained in the
 93 laboratory.



94
 95 **Fig2. Preparation process of esterified BF**

96 **2.2 Preparation of esterified BF**

97 A select quantity of BF was treated with 1 wt% NaOH solution for 24 h, washed repeatedly
 98 with tap water until the wash water pH was neutral and then dried in an oven of 60°C to constant
 99 weight (Fig.2). Next, 30 g of the alkali-treated BF (dry base) was mixed with 4.5 g of LA and 0.9
 100 g of stannous octanate or with 4.5 g of MAH and then placed in a hydrothermal reaction kettle at

101 80°C for 2 h. The reaction products were cooled to room temperature, a select quantity of acetone
102 added, stirred for a while, and then the solvents removed by rotary evaporation. Finally, the
103 product was washed three times with acetone and placed into a 50°C oven and dried until constant
104 weight was achieved.

105 **2.3 Properties and characterization**

106 **2.3.1 Fourier-transform infrared spectroscopic analysis**

107 Chemical changes in esterified BF after esterification were characterized using
108 Fourier-transform infrared spectroscopy (FT-IR) of samples tabletted with KBr and (IRAffinity-1,
109 Shimadzu Corp., Kyoto, Japan). To remove moisture completely, native and esterified BF were
110 further dried in a muffle oven at 50°C for 48 h. Samples for testing were obtained by grinding
111 material fully with a weight ratio of sample/KBr of 1/100. FT-IR curves of samples were obtained
112 in a range of 400–4000 cm⁻¹.

113 **2.3.2 Determination of esterification degree**

114 First, 1.00 g of dry esterified BF was weighed and placed in a 250 mL conical flask. Next, 10
115 mL of 75% ethanol solution in deionized water was added, followed by the addition of 10 mL of
116 0.5 M aqueous sodium hydroxide solution. The stoppered conical flask was agitated, warmed to
117 30°C, and stirred for 1 h. Excess alkali was then neutralized with a standard 0.5 M aqueous
118 hydrochloric acid solution. A blank titration was performed using native BF and the degree of
119 esterification (DS) calculated as follows.

$$120 \quad W = \frac{Mc(V_0 - V_1)}{1000 \times nm} \times 100\%$$

$$121 \quad GR = \frac{162W}{M \times (100 - W)} \times 100\%$$

122 where W is the substituent group content, %; M the esterifying agent molecular weight, g; c the
123 aqueous hydrochloric acid solution concentration, M; V_0 the aqueous hydrochloric acid solution
124 volume consumed by the blank sample, mL; V_1 is the aqueous hydrochloric acid solution volume
125 consumed by the esterified BF sample, mL; n the number of hydrophobic groups from the grafted
126 monomer; and m the sample mass, g.

127 **2.3.3 Determination of water absorption**

128 To determine the effects of esterification on BF hydrophobicity, 2.0 g of native BF and

129 esterified BF (dry base) were separately placed in glass dishes that contained a set amount of water.
130 Over the test period, sample weights were measured every 24 h and water absorption calculated as
131 follows.

132

$$\text{water absorption} = \frac{W_t - W_0}{W_0} \times 100\%$$

133 where W_t is the sample weight after water absorption for t h and W_0 the sample weight when it
134 reached a constant dry weight.

135 **2.3.4 Contact angle measurements**

136 A set amount of native and esterified BF were weighed and pressed into pie-shaped samples 1.5
137 cm in diameter using a press machine with a pressure of 20 MPa. An optical contact angle
138 measurement instrument (OCA20, DataPhysics Instruments GmbH, Filderstadt, Germany) was
139 used to measure the sample contact angle, using distilled water as the test solution. For each
140 measurement, a 4-uL drop of water was placed on a test sample using a microsyringe and the
141 contact angle values measured to within 1°.

142 **2.3.5 Scanning electron microscopic analysis**

143 The morphologies of the native and esterified BF were determined with a scanning electron
144 microscope (SEM; Quanta 200, FEI Co., Hillsboro, OR, USA), operating at an acceleration
145 voltage of 20 kV. BF samples were mounted on circular aluminum stubs with double-sided
146 adhesive tape and coated with gold before testing.

147 **2.3.6 X-ray diffraction analysis**

148 Native and esterified BF were further dried in a vacuum oven at 50°C for 48 h to remove
149 remaining moisture. Sample crystallinity indices were measured using an X-ray diffractometer
150 (XRD; XD-2, Beijing Purkinje General Instrument Co., Ltd., Beijing, China) with a Cu target at
151 36 kV and 20 mA. Samples were tested in the angular range of $2\theta = 5\text{--}40^\circ$ with a scanning rate of
152 $4^\circ/\text{min}$. The empirical crystallization index Crl , proposed by Segal (Segal *et al.*, 1959), is a
153 measure of natural cellulose crystallinity [13]. The calculation for this is

154

$$Crl = \frac{I_{002} - I_{\text{amorph}}}{I_{002}} \times 100\%$$

155 where I_{002} is the maximum diffraction peak intensity of the main crystallization peak 002 and
156 I_{amorph} the diffraction intensity of 2θ angles to 18° .

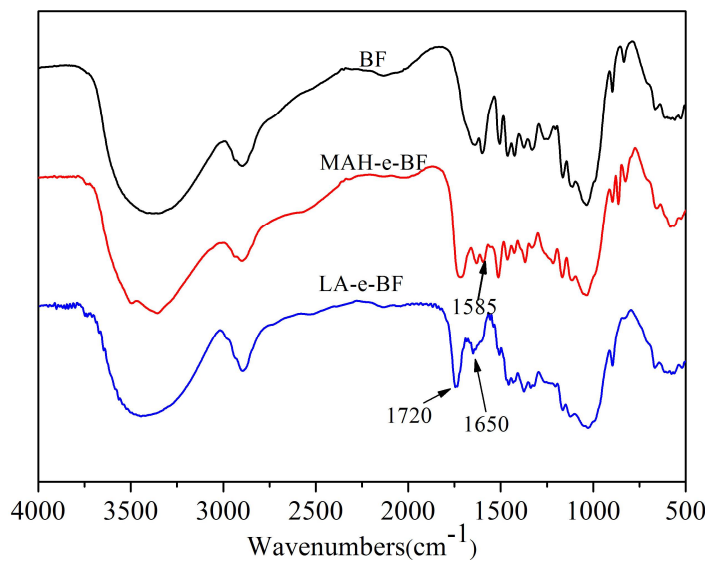
157 **2.3.7 Thermogravimetric analysis**

158 Thermogravimetric analytical (TGA) measurements of native and esterified BF were
159 performed using a 209 F3 TGA instrument (Netzsch Instruments Inc., Burlington, MA, USA).
160 About 5 mg of dried sample powders were placed in a platinum crucible and heated from 30 to
161 600°C at the rate of 10°C/min. Nitrogen dynamic carrier gas was applied at 30 mL/min.

162 **3 Results and Discussion**163 **3.1 *In situ* solid phase polymerization confirmation**

164 Esterification reactions between the esterifying agents and BF involved the hydrophilic
165 hydroxyl group (-OH) in BF being replaced by hydrophobic modifying groups (Fig.1). After
166 esterification with MAH, BF molecules were connected to C=O and C=C, and after the
167 esterification with LA, BF molecule were connected to C=O. FTIR analyses of native and
168 esterified BF were performed to verify that esterification had occurred and to investigate the
169 resulting chemical changes (Fig.3).

170 In unmodified BF, its basic compositional unit is *D*-anhydroglucose, of which the main
171 characteristic functional groups were C₂ and C₃-linked secondary hydroxyls and C₆-linked
172 primary hydroxyls and *D*-pyranose ring structures. The absorption peaks for these main structures
173 are shown in Fig.3. The characteristic peak centered at 3310 cm⁻¹ corresponded to O-H stretching
174 and vibration of hydrogen bond associations, 2930 cm⁻¹ to C-H asymmetrical stretching and
175 vibration, 1635 cm⁻¹ from the water tightly bound to the starch, 1152 cm⁻¹ from C-O-C
176 asymmetrical stretching and vibration, 1080 cm⁻¹ assigned to *D*-glucopyranose and
177 hydroxyl-linked C-O stretching and vibration, and 925 cm⁻¹ due to glucosidic bond vibration. In
178 the infrared spectrum of MAH-e-BF, in addition to all the characteristic absorption peaks of the BF,
179 the C=O absorption peak appeared at 1720 cm⁻¹ [14,15], and the C=C absorption peak appeared at
180 1585 cm⁻¹ [16]. LA-e-BF also showed a C=O absorption peak at 1720 cm⁻¹. Following
181 esterification with a BF-esterifying agent, unreacted MAH and LA and oligomer were removed by
182 acetone wash. This result confirmed that MAH and LA molecular chains were detected in the BF
183 skeleton, thus verifying that esterification had occurred between the BF and MAH or LA. The
184 solution titration results established that the degrees of substitution of MAH-e-BF and LA-e-BF
185 were 21.04 and 14.36%, respectively.

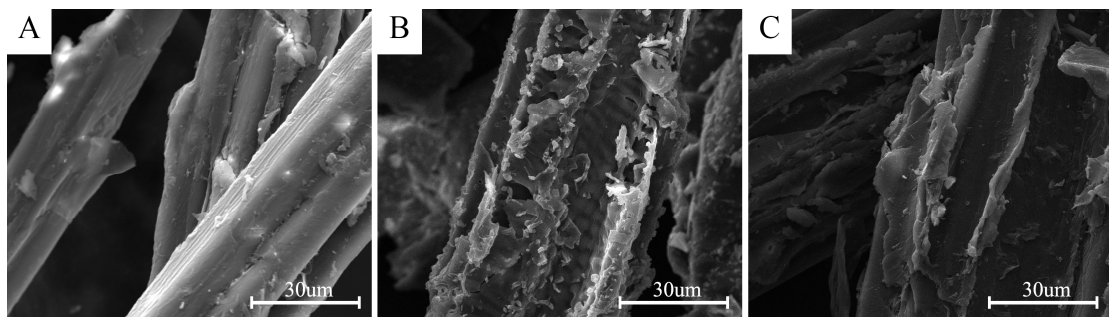


186

187 **Fig.3 Infrared spectrogram of BF, MAH-e-BF and LA-e-BF**188 **3.2 Morphology change of esterified BF**

189 SEM, in principle, uses a very fine focused high-energy electron beam to scan a sample and
 190 stimulate and collect a variety of physical information and, by accepting, amplifying and
 191 displaying this information, the surface morphology of a test specimen is observed. The surface
 192 morphology changes of native BF, MAH-e-BF, and LA-e-BF were observed by SEM to study the
 193 extent of changes in BF surface morphology as a result of the esterification reactions (Fig.4).

194



195

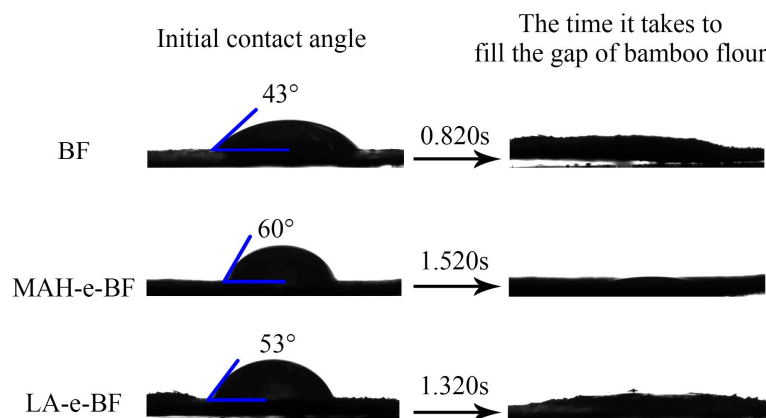
Fig.4 SEM images of NF (A), MAH-e-BF (B) and LA-e-BF (C)

196 The surface of native BF was smooth, with few trench, and low angles (Fig.4). Compared
 197 with native BF, esterified BF surfaces were fragmentary, rough, angular, and convex. Moreover,
 198 the covering material produced by these reactions were clearly observed on these surfaces, with
 199 the surface roughness and bonding degree of MAH-e-BF clearly greater than that of LA-e-BF.
 200 These results also indicated that BF surface roughness was positively correlated with the DS. SEM
 201 test results further showed that MAH and LA were successfully reacted with BF by this *in situ*
 202 solid-phase esterification method, with the resulting effects from MAH-modification appearing to

203 be better than with LA.

204 3.3 Water resistance of esterified BF

205 The BF molecular chain contains hydrophilic hydroxyl groups, which exhibit hydrophilic
206 properties [17]. In this experiment, *in situ* solid-phase esterification of MAH and LA replaced
207 hydroxyl groups on BF with hydrophobic groups, which resulted a reduction of the number of
208 hydrophilic hydroxyl groups and concomitant increase in the number of hydrophobic groups, thus
209 enhancing BF hydrophobicity. This phenomenon was verified by analyzing MAH-e-BF and
210 LA-e-BF hydrophobicity using contact angle measurements. The water contact angle on a surface
211 is the angle formed by a tangent line from the water droplet to a solid surface and is an indication
212 of the relative sample-surface hydrophobic character. The larger the contact angle, the higher the
213 material's hydrophobicity [18]. Native BF, MAH-e-BF, and LA-e-BF were tested using a contact
214 angle tester (Fig.5).



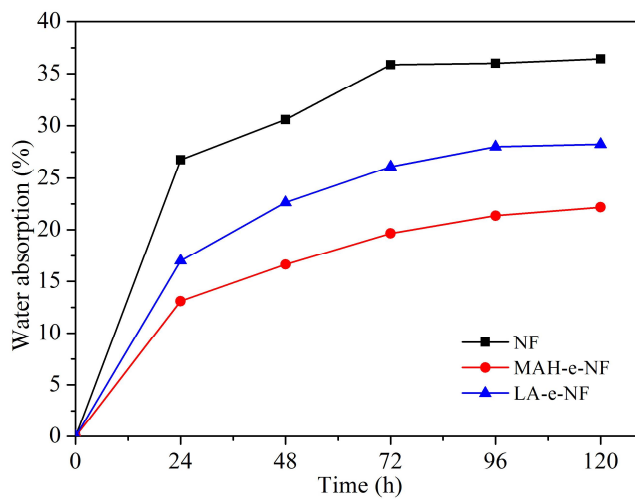
215

216 **Fig.5 The contact angle of BF, MAH-e-BF and LA-e-BF**

217 The initial contact angle of the BF was only 43° and full absorption of water droplets
218 required only 0.820 s. After *in situ* modification by solid phase esterification, the initial contact
219 angle increased and the full absorption time of water droplets was prolonged for both MAH-e-BF
220 and LA-e-BF (Fig.5). The results suggested improved hydrophobicity in the esterified BF
221 compared to native BF. The reasons for this phenomenon included the replacement of hydrophilic
222 hydroxyl groups on BF with hydrophobic groups, resulting the hydrophobic properties of
223 modified BF clearly improving. SEM analysis had shown that, after BF esterification with MAH
224 or LA, BF surfaces were coated to a certain extent, reducing their water absorption capacity.
225 MAH-e-BF exhibited the greater contact angle and longer absorption time, compared to those of

226 LA-e-BF, indicating that MAH-e-BF hydrophobicity was better than LA-e-BF. The
227 hydrophobicity of esterified BF was directly related to the number of hydrophobic groups grafted
228 to BF and more hydrophobic groups resulted in better hydrophobicity. Thus, the measured contact
229 angles were consistent with the DS. This was in line with the results from SEM analyses.

230 Improvement in BF hydrophobic properties of BF by ester-modification was confirmed by
231 determining the water absorption of BF, MAH-e-BF, and LA-e-BF based on their relative weight
232 change after exposure to water (Fig. 7). Native BF water absorption gradually increased over time,
233 but water absorption by MAH-e-BF and LA-e-BF were both lower than that of BF during soaking
234 for 120 h, which further demonstrated that the esterification significantly improved the water
235 resistance in modified BF. Comparison of water absorption for the two esterified BF revealed that
236 MAH-e-BF was lower than LA-e-BF. Thus, the hydrophobicity of MAH-e-BF was found to be
237 better than that of LA-e-BF, which was in agreement with contact angle test results.

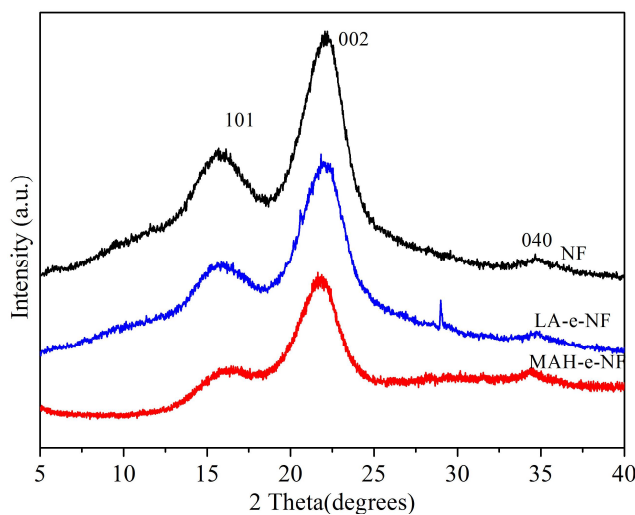


238
239 **Fig.6 Scatter diagram of water absorption change of BF, MAH-e-BF and LA-e-BF**

240 **3.4 Crystalline structural changes of esterified BF**

241 As BF crystal structure was easily affected by high temperatures and reactions with an
242 esterifying agent, the crystal structure of BF, MAH-e-BF, and LA-e-BF were analyzed by XRD
243 (Fig. 7). XRD diffraction peaks for native BF were a typical of $I\beta$ type crystalline structures,
244 whose 2θ values were 16.25, 22.47, and 33.85°, which corresponded to diffraction peaks of the
245 101, 002, and 040 crystal faces, respectively [19]. After esterification modification, the diffraction
246 peaks of the main crystal faces 101, 002, and 040 of MAH-e-BF and LA-e-BF were similar to
247 those of BF. This result showed that esterification occurred mainly in noncrystalline regions of BF,
248 because the changes in the materials' crystalline region were very small. However, XRD

249 diffraction peak intensities from MAH-e-BF and LA-e-BF were clearly weaker than those of
250 native BF.



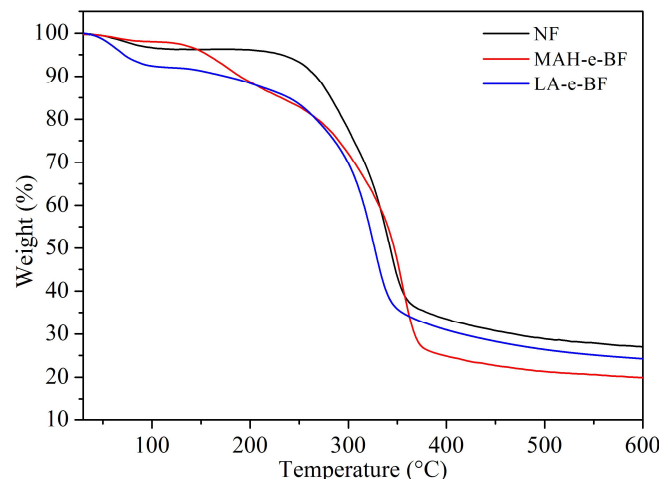
251

252 **Fig.7 X-ray diffraction pattern of BF, MAH-e-BF and LA-e-BF**

253 The BF crystallinity degree was calculated to be 56.78%, with the crystallinity of
254 MAH-e-BF and LA-e-BF found to be 47.45 and 51.07%, respectively, which showed that BF
255 crystallinity decreased after *in situ* solid phase esterification with MAH or LA. Because of this
256 treatment, MAH and LA infiltrated into the crystalline area and destroyed hydrogen bonding
257 between molecules in the crystalline region. At the same time, BF hydroxyl groups chain-reacted
258 with MAH or LA molecules and molecular chains gradually grew and crosslinked, which further
259 destroyed BF crystallinity. Conversely, destruction of the crystalline zone facilitated these
260 reactions, which led to a further decrease in crystallinity. As BF crystallinity decreased, the forces
261 between BF molecules were weakened [20], such that the thermal plasticity of MAH-e-BF and
262 LA-e-BF improved. MAH-e-BF crystallinity was less than that of LA-e-BF, owing to higher DS in
263 MAH-e-BF and more reacted BF chain hydroxyl groups, producing more serious destruction of
264 hydrogen bonds.

265 **3.5 Thermal performance analysis**

266 Based on XRD analysis of esterified BF, esterification were observed to decrease BF
267 crystallinity by changing the crystalline structure, which inevitably affected BF thermal properties.
268 Therefore, TGA of the material was used to determine thermal property changes in BF when it
269 was altered to form MAH-e-BF and LA-e-BF (Fig. 8).



270

271

Fig.8 TGA curves of BF, MAH-e-BF and LA-e-BF

272 Thermal degradation of native and esterified BF was divided into three stages, with
273 temperature ranges of 50–120, 120–400, and 400–600°C (Fig.8). The first stage represented water
274 evaporation from BF. In the second stage hemicellulose, cellulose, and some xylem in BF
275 thermally decomposed and the fastest decomposition rate was observed. In the third stage
276 (>400°C), the remaining material decomposed to carbon through broken chain pyrolysis. The
277 initiation temperatures of thermal decomposition in MAH-e-BF and LA-e-BF were clearly lower
278 than BF and the residual ratio also lower than BF. These results were attributed to decreased
279 crystallinity of MAH-e-BF and LA-e-BF from esterification and decreased in the of the BF
280 molecules. This result also suggested an increase in BF plasticity as a result of esterification.
281 Compared to MAH-e-BF and LA-e-BF, the thermal decomposition temperature and residual ratio
282 of MAH-e-BF was lower than those of LA-e-BF, which was due to their crystallinity degrees. This
283 also indicated that MAH-e-BF molecules were more loosely arranged and thus had better thermal
284 plasticity.

285 **4. Conclusions**

286 This study demonstrated the successful preparation of MAH-e-BF and LA-e-BF using an *in*
287 *situ* solid phase esterification method, achieving DS values at 21.04 and 14.36%, respectively.
288 Esterification resulted in the replacement of hydroxyl groups on BF *D*-anhydroglucose moieties
289 with hydrophobic groups from MAH or LA, which improved BF hydrophobic characteristics.
290 Esterified BF hydrophobicity was significantly higher than native BF and MAH-e-BF
291 hydrophobicity was better than LA-e-BF. Esterified BF surfaces were covered with graft polymer,
292 with the surface roughness and bonding degree of MAH-e-BF clearly greater than those of

293 LA-e-BF. The crystalline structure the esterified BF showed some damage, with the MAH-e-BF
294 exhibiting a greater decrease in crystallinity than LA-e-BF. Overall, esterification improved BF
295 thermoplasticity and MAH-e-BF thermoplasticity was better than LA-e-BF.

296 Esterified BF produced by *in situ* solid phase esterification exhibited increased overall
297 hydrophobicity with concurrent increased interface compatibility, allowing an expanded range of
298 applications in bamboo plastic composites. This work compared the influence of two esterifying
299 agents on BF esterification degree and hydrophobic character, providing reference data for the
300 preparation of blended composites of BF and other polymers.

301 Acknowledgments

302 This work was financially supported by the National Natural Science Foundation of China
303 (31600460), China Postdoctoral Science Fund Special Projects (2017T100615) and Innovation
304 and entrepreneurship project of college students in Hunan.

305 References

- 306 [1] Li, Y.J., Xu, B., Zhang, Q.S., Jiang, S.X., 2016. Present situation and the countermeasure
307 analysis of bamboo timber processing industry in China. *J. Forestry Eng.*, 2016, 1, 2-7.
- 308 [2] Huang, Y., Fei, B., Wei, P., Zhao, C., 2016. Mechanical properties of bamboo fiber cell walls
309 during the culm development by nanoindentation. *Ind. Crop. Prod.*, 92, 102-108.
- 310 [3] Nugroho, N., Ando, N., 2001. Development of structural composite products made from
311 bamboo II: fundamental properties of laminated bamboo lumber. *J. Wood Sci.*, 47, 237-242.
- 312 [4] Sun, S.L., Wen, J.L., Ma, M.G., Sun, R.C., 2014. Structural features and antioxidant activities
313 of degraded lignins from steam exploded bamboo stem. *Ind. Crop. Prod.*, 56, 128-136.
- 314 [5] Tung N H, Yamamoto H, Matsuoka T, et al. Effect of surface treatment on interfacial strength
315 between bamboo fiber and PP resin[J]. JSME International Journal Series A Solid Mechanics
316 and Material Engineering, 2004, 47(4): 561-565.
- 317 [6] Ashori A. Wood–plastic composites as promising green-composites for automotive industries
318 [J]. *Bioresource Technology*, 2008, 99(11): 4661-4667.
- 319 [7] Tokoro R, Vu D M, Okubo K, et al. How to improve mechanical properties of polylactic acid
320 with bamboo fibers[J]. *Journal of materials science*, 2008, 43(2): 775-787.
- 321 [8] Li W, Qiao X, Sun K, et al. Effect of electron beam irradiation on the silk fibroin fiber/poly
322 (ϵ -caprolactone) composite[J]. *Journal of applied polymer science*, 2009, 113(2): 1063-1069.

323 [9] Bledzki A K, Gassan J. Composites reinforced with cellulose based fibres[J]. *Progress in*
324 *polymer science*, 1999, 24(2): 221-274.

325 [10] Lee S H, Wang S. Biodegradable polymers/bamboo fiber bio-composite with bio-based
326 coupling agent[J]. *Composites Part A: Applied Science and Manufacturing*, 2006, 37(1):
327 80-91.

328 [11] Plackett D, Andersen T L, Pedersen W B, et al. Biodegradable composites based on
329 L-polylactide and jute fibres[J]. *Composites science and technology*, 2003, 63(9): 1287-1296.

330 [12] Avella M, Bogoeva - Gaceva G, Buzoarovska A, et al. Poly
331 (3 - hydroxybutyrate - co - 3 - hydroxyvalerate) - based biocomposites reinforced with
332 kenaf fibers[J]. *Journal of Applied Polymer Science*, 2007, 104(5): 3192-3200.

333 [13] Xue Z H, Zhao G J. Influence of different treatments of on wood crystal properties[J]. *Journal*
334 *of Northwest Forestry University*, 2007, 22(2): 169-171.

335 [14] Dontulwar J R, Borikar D K, Gogte B B. An esteric polymer synthesis and its
336 characterization using starch, glycerol and maleic anhydride as precursor[J]. *Carbohydrate*
337 *polymers*, 2006, 65(2): 207-210.

338 [15] Ma X, Chang P R, Yu J, et al. Preparation and properties of biodegradable poly (propylene
339 carbonate)/thermoplastic dried starch composites[J]. *Carbohydrate Polymers*, 2008, 71(2):
340 229-234.

341 [16] Tay SH, Pang SC and Chin SF. Facile synthesis of starch-maleate monoesters from native
342 sago starch. *Carbohydrate Polymers* 2012; 88: 1195-1200.

343 [17] Kushwaha P K, Kumar R. Influence of chemical treatments on the mechanical and water
344 absorption properties of bamboo fiber composites[J]. *Journal of Reinforced Plastics and*
345 *Composites*, 2011, 30(1): 73-85.

346 [18] Zeng J B, Jiao L, Li Y D, et al. Bio-based blends of starch and poly (butylene succinate) with
347 improved miscibility, mechanical properties, and reduced water absorption[J]. *Carbohydrate*
348 *Polymers*, 2011, 83(2): 762-768.

349 [19] Liu D, Zhong T, Chang P R, et al. Starch composites reinforced by bamboo cellulosic
350 crystals[J]. *Bioresource Technology*, 2010, 101(7): 2529-2536.

351 [20] Bajpai P K, Singh I, Madaan J. Development and characterization of PLA-based green
352 composites: A review[J]. *Journal of Thermoplastic Composite Materials*, 2014, 27(1): 52-81.